Thermal Response of Polycrystalline Diamond Compact Cutters Under Simulated Downhole Conditions

D.A. Glowka, Sandia Natl. Laboratories
C.M. Stone, Sandia Natl. Laboratories

Abstract

An analytical method is developed to predict temperatures in polycrystalline diamond compact (PDC) drag cutters under steady-state and transient downhole conditions. The method is used to determine mean wearflat temperatures for cutters under conditions used in previous experiments to measure cutter wear. A correlation between wearflat temperatures and cutter wear rates is demonstrated, and it is shown that, for the particular rock type tested, cutter wear rates increase significantly above 350°C [662°F]. The concept of a critical weight on bit, above which wearflat temperatures exceed this value, is introduced. The effects of several parameters on the critical WOB are examined. These include cutter thermal conductivity, diamond layer thickness, rock properties, convective cooling, bit balling, and transient events such as bit bounce. Preliminary results of thermal stress modeling show that plastic yielding of the cutter structure can occur under certain downhole conditions.

Introduction

Drill bits using PDC drag cutters have been used for the past few years with considerable success in the oil and gas drilling industry.[1-3] Such bits have been shown to be quite sensitive, however, to formation characteristics and operating conditions, and the economic success of a particular bit run is highly dependent on identifying appropriate drilling intervals and operating the bit within its limits. Our interest in PDC bit technology has been in determining the drilling potential of these bits in the more severe environments associated with geothermal resources. This paper addresses the thermal limitations of PDC bits in such environments and investigates the effects of design and operating parameters on these limitations.

The work reported in this paper is an extension of work reported earlier.[4] More generalized boundary conditions are used for the finite element thermal modeling of single PDC cutters. The results are used to demonstrate the apparent adverse effect of operating temperature on cutter wear rates. A more restrictive safe operating limit of 350°C [662°F] is proposed, rather than the 750°C [1,382°F] limit assumed in the earlier work.

Cutter Temperature Theory and Analysis

The thermal phenomena considered in this analysis are frictional heating and convective cooling of PDC cutters under downhole drilling conditions. Fig. 1 is a graphical representation of this process. Because of the relative motion between the cutter and the rock, frictional heat is generated at the interface. The total quantity of frictional heat per unit wearflat area per unit time is

$$Q=K_f W v/A_w. \quad \ldots\ldots\ldots\ldots\ldots\ldots\ldots\ldots (1)$$

Because of the intimate contact between the cutter and the rock, this heat flux is divided between the cutter, Q_1, and the rock, Q_f, according to the value of the energy partitioning fraction α:

$$Q_1=\alpha Q=\alpha K_f W v/A_w, \quad \ldots\ldots\ldots\ldots\ldots\ldots (2)$$

and

$$Q_f=(1-\alpha)Q=(1-\alpha)K_f W v/A_w. \quad \ldots\ldots\ldots\ldots (3)$$

The value of α depends on the relative thermal resistances of the cutter and the rock, which in turn depend on their thermal properties, convective cooling rates, cutting speed, and cutter geometry.

A measure of the thermal resistance of the rock is obtained from the literature. Jaeger[5] gives the solution for the mean temperature rise of the contact area between a sliding, square heat source and the surface of a semi-infinite slab as

$$\bar{T}_s-T_f=\frac{4Q_f}{3\sqrt{\pi}k_{hf}}\left(\frac{\alpha_f L}{v}\right)^{1/2}, \quad \ldots\ldots\ldots\ldots (4)$$

where k_{hf} and α_f are thermal properties of the rock, L is the wearflat length parallel to the cutting direction, and v is the cutting speed. Because of the intimate contact between the cutter and the rock, it may be assumed that

$$\bar{T}_w\cong\bar{T}_s. \quad \ldots\ldots\ldots\ldots\ldots\ldots\ldots\ldots (5)$$

Combining Eqs. 2 through 5 and assuming that the wellbore has been cooled by the drilling fluid such that $T_f\cong T_{fl}$, the general result is

$$\alpha=\left[1+\frac{\bar{T}_w-T_{fl}}{Q_1}\frac{3\sqrt{\pi}}{4}k_{hf}\left(\frac{v}{\alpha_f L}\right)^{1/2}\right]^{-1}. \quad \ldots (6)$$

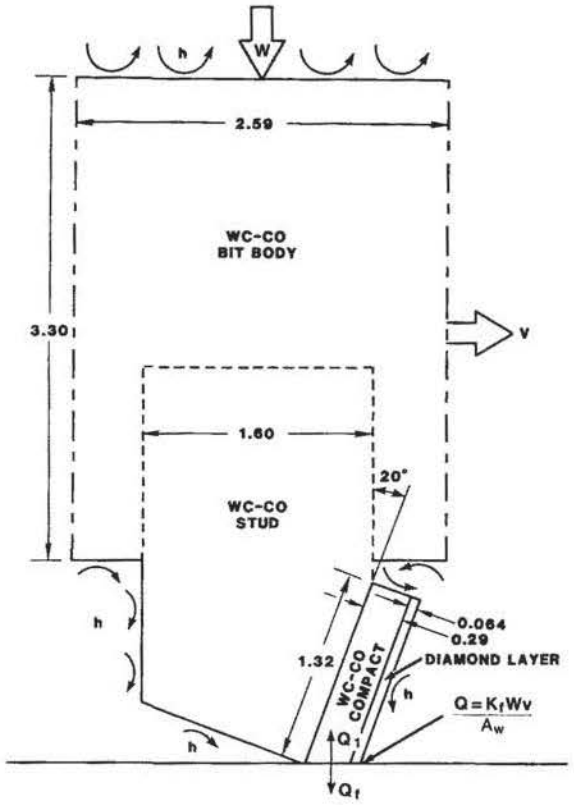

Fig. 1—Representation of phenomena modeled in baseline analysis.

For steady-state conditions, the ratio

$$f=\frac{\bar{T}_w-T_{fl}}{Q_1} \quad \ldots\ldots\ldots\ldots\ldots\ldots\ldots\ldots\ldots\ldots (7)$$

is known as the thermal response function for the cutter and may be determined with numerical modeling. The final equation for α under steady-state conditions is, therefore,

$$\alpha=\left[1+\frac{3\sqrt{\pi}}{4}fk_{hf}\left(\frac{v}{\alpha_f L}\right)^{1/2}\right]^{-1}, \quad \ldots\ldots\ldots\ldots (8)$$

as reported in Ref. 4. Transient effects on α will be discussed in a later section.

The function f is an effective thermal resistance of the cutter and is a complex function of cutter configuration, thermal properties, and cooling rates. Its value must be known to compute mean wearflat temperatures.

To determine f according to Eq. 7, cutter temperature distributions under simulated downhole conditions were computed with two-dimensional (2D) numerical models of the three cutter configurations shown in Fig. 2. The wearflat of the mildly worn cutter extends across the diamond layer of the PDC element. The wearflat of the moderately worn cutter includes the diamond layer and the tungsten-carbide-cobalt (WC-Co) compact to which the diamond is bonded. The severely worn cutter has a wearflat that extends well into the cutter stud. These three models thus span the range of cutter wear normally encountered in practice.

The portion of the numerical models surrounding the cutter stud represents approximately that segment of the bit body that is thermally affected by the single cutter. In other words, a full bit could be represented by a series of cutter models placed side by side. The vertical sides of the bit body segments thus are surfaces of approximate symmetry and are modeled as adiabatic for the baseline calculations. Different boundary conditions on these vertical surfaces are addressed in a later section. The upper surface of each model represents the inside cavity of the bit body and, therefore, is modeled as being convectively cooled. The bit body segments surrounding the cutters represent a generalization of the models used in the previous work,[4] where the tops of the cutter studs were assumed to be maintained at the fluid temperature.

Numerical simulation was performed with a 2D finite element code.[6] Steady-state solutions were obtained for

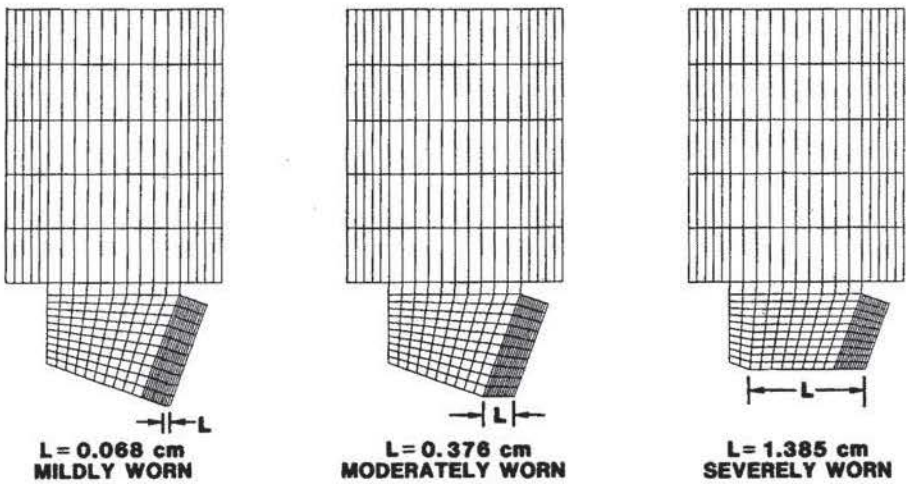

Fig. 2—Finite element meshes for the three cutter configurations studied.

TABLE 1—SUMMARY OF CONDITIONS FOR BASELINE STUDY (CASE 1)

Type of analysis	steady state
Stud material	Grade 55B WC-Co
k_h, W/cm·°C	0.8
ρ, g/cm^3	13.9
C, J/g·°C	0.23
WC-Co compact material	Grade 883 WC-Co
k_h, W/cm·°C	1.0
ρ, g/cm^3	15.0
C, J/g·°C	0.23
Bit body material	Grade 883 WC-Co
Diamond material	synthetic polycrystalline diamond
k_h,W/cm·°C	5.43
ρ, g/cm^3	3.51
C, J/g·°C	0.79
Diamond layer thickness, cm	0.064
k_{hf}, W/cm·°C	0.019
α_f, cm^2/s	0.01
T_{fl}, °C	50

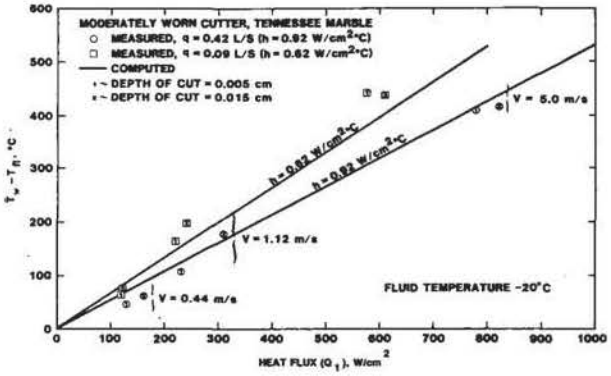

Fig. 3—Comparison of computed and measured wearflat temperatures (after Ref. 19).

each wear condition, assuming, for the baseline case, grade 55B WC-Co studs and grade 883 WC-Co compacts and bit bodies. The thermal properties used for these materials are shown in Table 1. The effects of different thermal conductivities also were investigated and are discussed in a later section.

For each wear condition, an arbitrary value of the wearflat heat flux Q_1 was used to compute the mean wearflat temperature rise for seven cutter surface cooling rates in the range h=0.01 to 10 W/(cm^2·°C) [18 to 1.8×10^4 Btu/(hr-sq ft-°F)]. These results were divided by Q_1 according to Eq. 7 to produce values of f as a function of heat transfer coefficient. The results are compiled in Table 2.

Substituting Eq. 2 into Eq. 7 produces an equation for predicting the mean wearflat temperature of a PDC cutter.

$$\bar{T}_w - T_{fl} = \frac{\alpha K_f W v}{A_w} f, \quad \ldots\ldots\ldots\ldots\ldots\ldots\ldots (9)$$

where α is determined from Eq. 8 and f is determined from the data in Table 2.

Available experimental temperature data obtained for PDC cutters under carefully controlled conditions[7] have been used to test the validity of Eq. 9. The measured values of mean wearflat temperature are shown in Fig. 3, together with the predictions of Eq. 9. The agreement is good enough for the predictive method to be used with confidence, at least for identifying trends. The effects of certain design and operating parameters on wearflat temperature manifest themselves in Eq. 9 through changes in the cutter thermal response function f. These effects are discussed in a later section in connection with the concept of critical weight on cutter (WOC).

Critical WOC

There are a number of ways in which Eq. 9 could be used, but perhaps the most useful is in estimating the maximum WOC that can be used in practice without causing an excessive rate of cutter wear. Eq. 9 shows mean wearflat

TABLE 2—SUMMARY OF STUDIED PARAMETERS AND NUMERICAL RESULTS

		Thermal Response Function, f (°C·cm^2/W)											
		Mildly Worn				Moderately Worn				Severely Worn			
		h (W/cm^2·°C)				h (W/cm^2·°C)				h (W/cm^2·°C)			
Case	Change From Baseline Analysis	0.01	0.10	1.0	5.0	0.01	0.10	1.0	5.0	0.01	0.10	1.0	5.0
1	None	0.956	0.170	0.064	0.035	5.46	0.896	0.325	0.198	23.5	3.22	0.924	0.599
2	Grade 78B WC-Co stud and bit body (k_h = 0.42)	0.988	—	0.066	—	5.68	—	0.370	—	24.5	—	1.34	—
3	Grade 78B WC-Co compact, stud and bit body (k_h = 0.42)	1.02	—	0.078	—	5.86	—	0.495	—	24.6	—	1.52	—
4	Thicker diamond layer (0.140 cm)	0.921	0.151	0.051	0.027	5.31	0.833	0.277	0.160	22.9	3.13	0.878	0.563
5	Cooling of vertical bit body surfaces	0.585	—	0.064	—	3.21	—	0.322	—	12.2	—	0.883	—
6	Internal cooling of cutter	—	—	—	—	5.27	—	0.325	—	—	—	—	—
7	Higher (k_{hf} = 0.05) and lower (k_{hf} = 0.006) rock thermal conductivity	—	—	—	—	—	—	—	—	—	—	—	—
8	T_{fl} = 50 to 150°C	—	—	—	—	—	—	—	—	—	—	—	—
9	Lower x% of diamond face insulated from fluid:												
	x = 20	0.991	—	0.075	—	5.65	—	0.363	—	24.2	—	0.973	—
	x = 50	1.05	—	0.082	—	5.95	—	0.402	—	25.3	—	1.05	—
10	Transient analysis (beginning to drill) v = 1 m/s; $T_i = T_{fl}$ = 100°C; $\bar{T}_{wss}$ = 700°C.												
11	Transient analysis (lifting bit off bottom) v = 1 m/s; T_{fl} = 100°C; $\bar{T}_{wi}$ = 700°C.												
12	Transient analysis (bit bounce); v = 1 m/s; T_{fl} = 100°C; $\bar{T}_{wi}$ = 300°C; bounce frequency = 5 cycles/sec.												

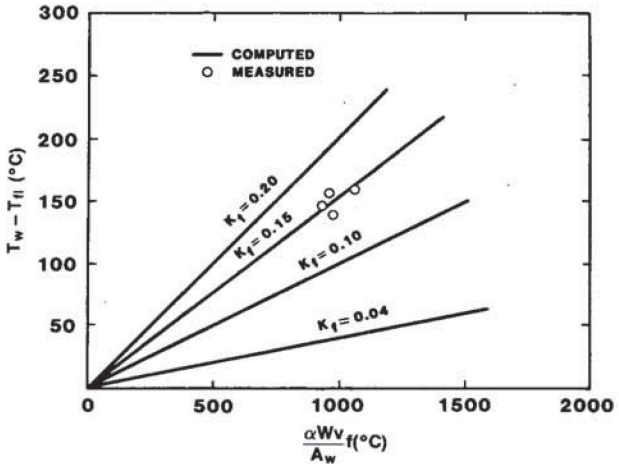

Fig. 4—Data used to determine PDC-sandstone friction coefficient with water/oil coolant.

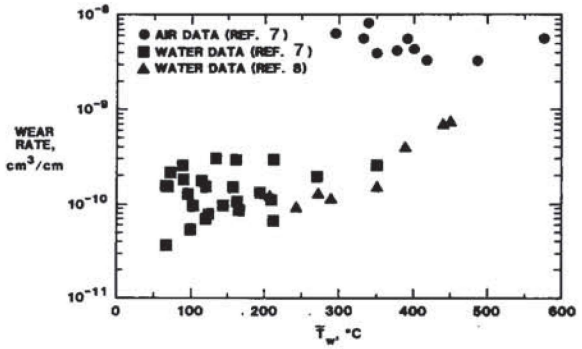

Fig. 5—Experimental wear rates as a function of computed wearflat temperature (volume of wear/length of cut).

temperature rise to be directly proportional to WOC. If high wearflat temperatures lead to increased cutter wear rates, then we should expect bit life generally to be reduced at higher WOB. Since penetration rate generally increases with WOB, this suggests a trade-off between bit life and penetration rate.

As noted in Ref. 8, the primary mode of wear of PDC cutters below wearflat temperatures of 750°C [1,382°F] is microchipping of individual diamond grains in the diamond layer. Above 750°C [1,382°F], the wear mode changes to a more severe form in which thermal effects weaken diamond bonds and whole-grain pullout occurs. Thus, it is obvious that the cutter wearflat temperature should be maintained below 750°C [1,382°F] to prevent catastrophic wear rates. It will be shown, however, that cutter wearflats probably should be maintained at a lower temperature to prevent inordinately rapid wear in even the microchipping mode.

In laboratory cutting of Jackfork sandstone, the wear rate of PDC cutters has been shown to be a function of cutter speed.[8] It was suggested that this increase is caused by the fact that higher sliding speeds cause elevated wearflat temperatures, which in turn cause a decrease in the hardness of individual diamond crystals. Tungsten carbide also experiences a drop in hardness with increasing temperature.[9] Since abrasive wear of cutting tools primarily depends on the relative hardness of the cutter and the material being cut,[10] a relative decrease in cutter hardness will cause an increase in the failure rate of asperities on the cutter surface and, hence, a higher wear rate. This hypothesis is supported by the conclusions of metal machining research, which show that the wear of machine tools is strongly temperature dependent,[10] even though other factors such as workpiece characteristics do play a role.[11]

TABLE 3—MEASURED PDC FRICTION COEFFICIENTS[7]

Rock Type	Speed (m/s)	Friction coefficient, η_f Water	Mud	Diesel	Air
Marble	1	0.20	0.17	0.34	0.33
	5	0.15	0.11	0.13	0.15
Sandstone	1	0.03	0.04	0.05	0.10
	5	0.05	0.04	0.30	0.30
Granite	1	0.09	—	—	0.18
	5	0.05	—	—	0.14
Shale	1	0.09	—	—	0.18
	5	0.06	—	—	0.15

Assuming that wearflat temperature is a controlling factor in cutter wear rate for at least a given rock type, it would be useful to correlate experimental wear rates with computed wearflat temperatures under the same conditions. Two sources of experimental data are available. In the first,[8] Jackfork sandstone was cut at atmospheric pressure with a jet of 40:1 water:oil coolant directed at the cutter face (0.41 L/s [6.5 gal/min] flow rate). In the second,[7] Nugget sandstone was cut, both with and without this coolant. Cutter wear data were obtained at a fixed depth of cut of 0.05 cm [0.02 in.], with cutting speed ranging from 0.53 to 3.25 m/s [1.7 to 10.7 ft/sec].

All the parameters required by Eq. 9 to compute wearflat temperatures were recorded in these tests, with the exception of the friction coefficient with the water:oil coolant. This can be determined indirectly from cutter wearflat temperature measurements in which the same type coolant (40:1 water:oil) and Nugget sandstone were used.[7] Fig. 4 shows wearflat temperature rise as a function of a group of measured and computed variables, with the friction coefficient as a parameter. The computed temperature rise agrees with the experimental data when a friction coefficient of K_f=0.15 is assumed.

By using this value for K_f with the coolant and using the air/sandstone data of Table 3 for K_f with the dry tests, the mean wearflat temperatures corresponding to the experimental conditions for the wear tests are computed and shown in Fig. 5. The results indicate that wear rates under dry cutting conditions are one to two orders of magnitude higher than those obtained with cooling and lubrication. Fig. 5 further shows that even with cooling and lubrication, wear rate begins to increase significantly above a temperature of approximately 350°C [662°F] (note the data of Ref. 8). Although other surface properties affected by cutter environment undoubtedly play a role in controlling cutter wear, these data lend support to the suggestion that temperature effects on wearflat hardness may be a leading cause of the increased wear rates.

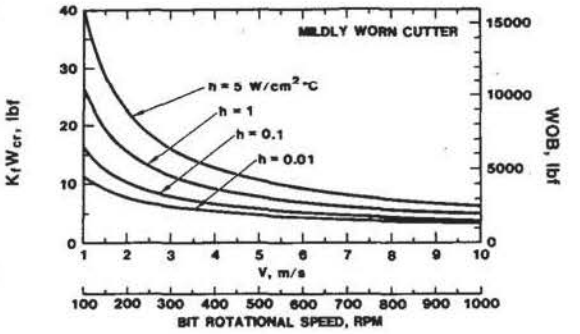

Fig. 6—Critical WOC for the mildly worn cutter under baseline conditions.

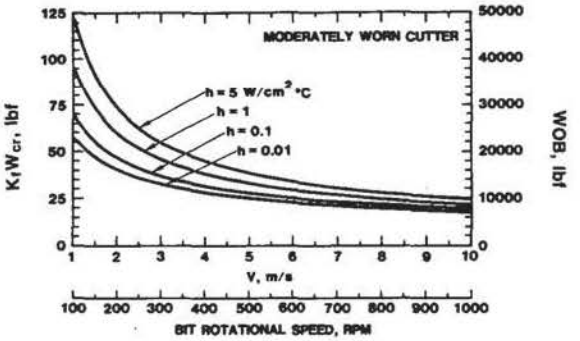

Fig. 7—Critical WOC for the moderately worn cutter under baseline conditions.

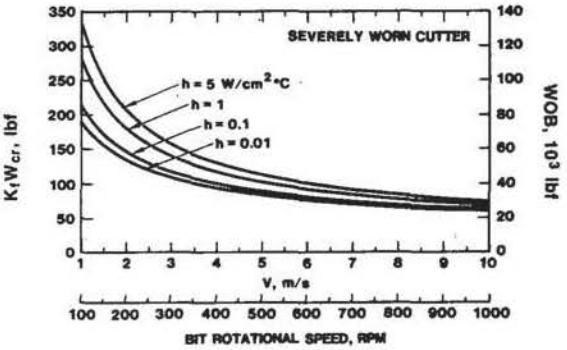

Fig. 8—Critical WOC for the severely worn cutter under baseline conditions.

Although admittedly based on limited data for a single family of rock, we will assume for discussion purposes that 350°C [662°F] is the critical mean wearflat temperature, above which wear rate increases dramatically. The trends observed as a result of this assumption will be valid even if the magnitude of the critical temperature is somewhat in error.

The critical WOC now can be derived by solving Eq. 9 for W at the critical wearflat temperature:

$$W_{cr}=\frac{A_w}{\alpha f K_f v}(\bar{T}_w-T_{fl})_{cr}. \quad \ldots\ldots\ldots\ldots\ldots\ldots (10)$$

For purposes of illustration, a typical downhole fluid temperature of $T_{fl}=50$°C [122°F] is assumed for the baseline case. The effects of downhole fluid temperature are discussed later. To illustrate the effects of various parameters on the critical WOC, Eq. 10 is plotted in the form,

$$K_f W_{cr}=\frac{300A_w}{\alpha f v}. \quad \ldots\ldots\ldots\ldots\ldots\ldots\ldots (11)$$

Values for the wearflat area A_w are required to plot Eq. 11 for the three wear conditions evaluated in this study. As shown in the Appendix, the computed wearflat area for a −20° backrake, stud-mounted PDC cutter is given approximately by the equation

$$A_w=0.82L^{1.48}. \quad \ldots\ldots\ldots\ldots\ldots\ldots\ldots (12)$$

The values of f used in Eq. 11 were taken from Table 2 for the baseline case. Eq. 8 was used to compute α. The results are presented in Figs. 6, 7, and 8, respectively, for the mildly, moderately, and severely worn cutters. The scales on the right side of these graphs represent the total WOB for a 22.2-cm [8.75-in.] bit with 40 cutters, assuming a friction coefficient of 0.10. The lower horizontal scales represent the bit rotational speed corresponding to v, assuming the cutter to be near the periphery of a 22.2-cm [8.75-in.] bit.

The curves of Figs. 6 through 8 show the effects of convective cooling on the critical WOB. The higher cooling rates associated with water drilling, $h=0.1$ to 1.0 W/(cm^2·°C) [180 to 1800 Btu/(hr-sq ft-°F)] allow a much greater cutter weight to be used than those associated with air drilling, $h=0.01$ to 0.1 W/(cm^2·°C) [18 to180 Btu/(hr-sq ft-°F)], especially at the lower cutter speeds. This detrimental effect of air drilling is compounded by the fact that friction coefficients are generally higher with air than with water, as noted in Table 3. Convective cooling effects are discussed further in a later section.

Comparing the curves of Figs. 6 through 8 shows that higher bit weights can be used as the cutters wear. This suggests that under certain operating conditions, reduced WOB should be used when the cutters are sharp to prevent thermal damage and, consequently, unacceptably high wear rates.

In the following sections, the effects of several design, operating, and environmental parameters on critical WOC are examined and compared with the baseline calculations. A summary of all parameters investigated is given in Table 2.

Effects of Cutter Design

Cutter Thermal Conductivity. The first cutter design change studied relates to the materials used to construct the cutter stud and bit body. The WC-Co grades assumed for these components in the baseline analysis, Case 1, have thermal conductivities that are among the highest of all WC-Co grades used in rock mining applications. The effects of using materials with lower conductivities were studied. In Case 2, the thermal effects of using Grade 78B

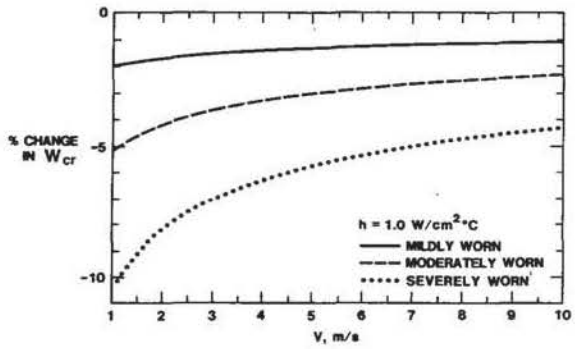

Fig. 9—Effects of using a WC-Co grade with lower thermal conductivity for the cutter stud and bit body; Case 2, $h = 1.0$ W/(cm^2 · °C).

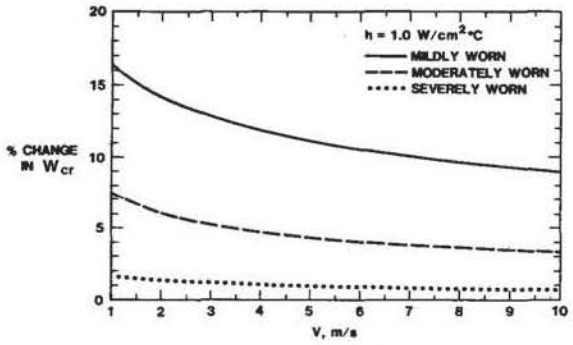

Fig. 10—Effects of thicker diamond layer: Case 4, $h = 1.0$ W/(cm^2 · °C).

WC-Co for the cutter stud and bit body are addressed, and the results are shown in Fig. 9 for a cooling rate typical of water drilling. Assuming the critical wearflat temperature of various WC-Co grades to be approximately the same, Fig. 9 shows that bit weight for a given drilling environment must be reduced if the WC-Co grade assumed in Case 2 is used, rather than the grade assumed in the baseline analysis. The change is significant only for the severly worn tool (-10% at $v = 1$ m/s [3.3 ft/sec]). This is because heat transfer in the mildly and moderately worn cutters is primarily controlled by the thermal conductivity of the diamond and WC-Co compact, which remained unchanged in the Case 2 analysis.

The effects of also changing the WC-Co compact to a grade of lower conductivity are addressed in Case 3. In this case (not illustrated), the detrimental effects on W_{cr} for the mildly and moderately worn cutters are comparable to those for the severly worn cutter in Fig. 9. In both the Case 2 and Case 3 analyses, the detrimental effects of low cutter material thermal conductivity are negligible with typical air-drilling cooling rates because thermal convection, not conductivity, is the controlling factor at low cooling rates.

Steel cutter studs have been used in PDC bits in the past. The thermal conductivity of steel is comparable to that of the WC-Co grade assumed in Case 2. The thermal effects of using steel thus would be comparable to those seen in Fig. 9; that is, a severely worn cutter at $v = 1$ m/s [3.3 ft/sec] would experience a mean wearflat temperature rise about 10% higher than that computed for the baseline analysis. Since the wear resistance of steel is much lower than that of tungsten carbide, however, a much larger decrease in critical WOC should be expected when using steel studs.

Diamond Layer Thickness. The effects of using a thicker diamond layer than normally is used on PDC cutters are addressed in Case 4. Here, the cutters were modeled with a 0.140-cm [0.055-in.] thick diamond layer, compared with the 0.064-cm [0.025-in.] diamond layer modeled in the baseline case. The beneficial effects of the thicker diamond layer are shown in Fig. 10 for a cooling rate typical of water drilling. As expected, the effects are largest for the mildly worn cutter and negligible for the severely worn cutter. At $v = 1$ m/s [3.3 ft/sec], up to 16% more WOB can be used with a mildly worn cutter if the thicker diamond layer is used. With cooling rates typical of air drilling, essentially no effects are observed; however, with any cooling rate, PDC elements with such thicker diamond layers may have inherently longer lives, since a larger fraction of a given wearflat would be composed of diamond, which is more wear resistant than WC-Co.

Hydraulic Design. Two parameters of hydraulic design were studied in Cases 5 and 6. In Case 5, cooling is imposed on the vertical sides of the bit body segments that were modeled as adiabatic in the baseline case. This simulates the placement of fluid ports or nozzles through the bit body at these locations. The values of f obtained for Case 5 are tabulated in Table 2 and show that under low cooling conditions the temperature rise for a given wearflat heat flux is about one-half that for the baseline case. It should be noted, however, that the temperature rise as given in Eq. 9 depends on the product of αf, where α, in turn, is a function of f. The decreased values of f for Case 5 cause an increase in α for all three cutters. In other words, nozzle cooling of the bit body causes an increased fraction of the total frictional heat to flow into the cutter. The net result is that the product of αf and, hence, the critical WOC remain almost the same as those computed for the baseline case. In fact, with typical air-drilling cooling rates, a maximum increase in critical WOC of only 6% at $v = 1$ m/s [3.3 ft/sec] was computed for the mildly worn cutter with nozzle cooling of the bit body. For higher cooling rates or greater cutter wear, the results are almost identical to those of the baseline case. These results provide a further indication that cutter wearflat temperatures are controlled primarily by conditions near the wearflat.

In Case 6, the effects of internally cooling the cutter are examined. A 0.64-cm [0.25-in.] diameter fluid port through the cutter was modeled for the moderately worn case, as shown in Fig. 11. The internal surfaces of the port were convectively cooled with the same assumed heat transfer coefficient as the exterior surfaces of the cutter.

Surprisingly, inner cooling of the cutter hardly affects the values of the thermal response function f, as seen in Table 2. This apparently is a result of the dominant effect of conditions nearer the wearflat. No attempts were made to evaluate a model with a fluid passage closer to

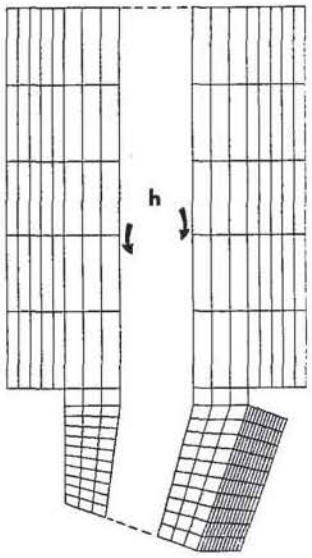

Fig. 11—Finite element mesh for studying the effects of cutter inner cooling.

the wearflat, since such a design would require the passage to curve inside the cutter, resulting in mud erosion and, consequently, structural weakening of the cutter.

Effects of Formation Characteristics

Friction Coefficient. Eq. 10 shows critical WOC to be inversely proportional to the coefficient of friction between the cutter and the rock. Although experimental data for friction coefficient under simulated downhole conditions are not available, data for PDC cutters have been obtained for a variety of rocks and coolant types under atmospheric pressure.[7] These data are compiled in Table 3 for reference. The major deficiency of these data is that they were obtained by sliding a cutter repeatedly over a circular path without actually cutting the rock. Under certain conditions, changes in rock surface characteristics were noted that might not have occurred if new rock surface were being exposed continuously by cutting. Nevertheless, these data are the best estimates available at this time. Note that the friction coefficient under these conditions is generally higher with air cooling than with liquid cooling, and it generally increases with cutting speed, though this is not always the case.

Rock Thermal Conductivity. Rock thermal conductivity affects cutter wearflat temperatures by affecting the fraction of frictional heat absorbed by the rock. Ref. 12 contains an extensive compilation of thermal conductivities for most rock types encountered in drilling. These data range from 0.006 W/(cm^2 · °C) [0.35 Btu/(hr-ft-°F)] for certain shales to over 0.05 W/(cm^2 · °C) [2.9 Btu/(hr-ft-°F)] for anhydrite and are affected by factors such as quartz content, porosity, and saturation.

The effects of rock thermal conductivity are addressed in Case 7 and illustrated in Fig. 12 for a typical water-cooling rate. In this case, both a higher and lower rock thermal conductivity are assumed: k_{hf}=0.05 W/(cm^2 · °C) [2.9 Btu/(hr-ft-°F)], a typical value for

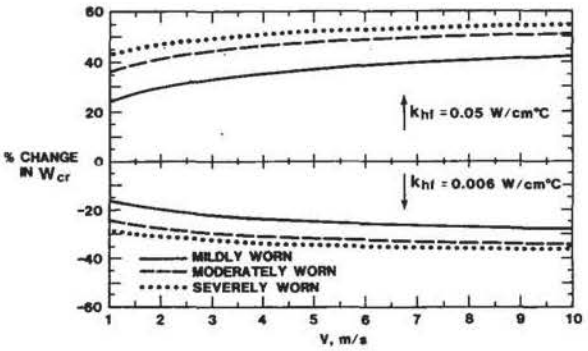

Fig. 12—Effects of higher and lower rock thermal conductivities: Case 7, h=1.0 W/(cm^2 · °C).

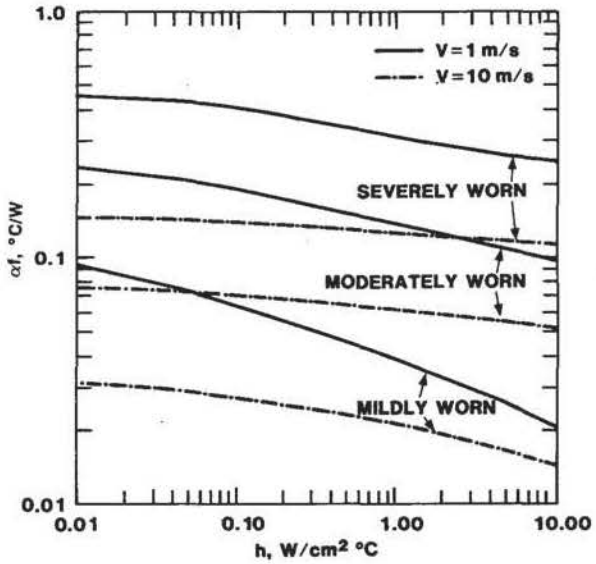

Fig. 13—Product αf as a function of cooling rate under baseline conditions.

anhydrite, and k_{hf}=0.006 W/(cm^2 · °C) [0.35 Btu/hr-ft-°F)], a low value for shale. Note that the effects on critical WOC are large, up to 42% at v=1 m/s [3.3 ft/sec] for the severely worn cutter. Similar effects are observed with the lower cooling rates typical of air drilling. These large effects are an indication that thermal properties of the formation being drilled must be known accurately if downhole cutter temperatures or critical WOB are to be predicted accurately. Since this is not usually possible, the results of this paper should be used primarily to determine trends and identify important variables.

Effects of Operating Conditions

Cutter Cooling Rate. Convective cooling plays a significant role in defining cutter thermal response and, hence, wearflat temperatures and critical WOB. These effects are illustrated in Figs. 6 through 8, where it is seen that the convective heat transfer coefficient has a larger effect on sharp cutters than worn ones, and the effects tend to decrease with increasing cutter speed. The thermal

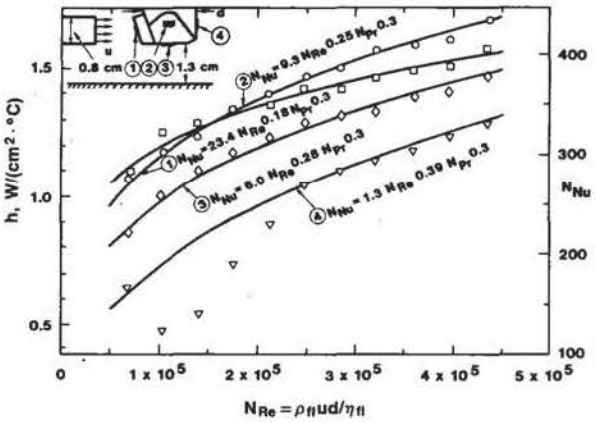

Fig. 14—PDC cutter heat transfer coefficients with impingement by a low-pressure water jet.

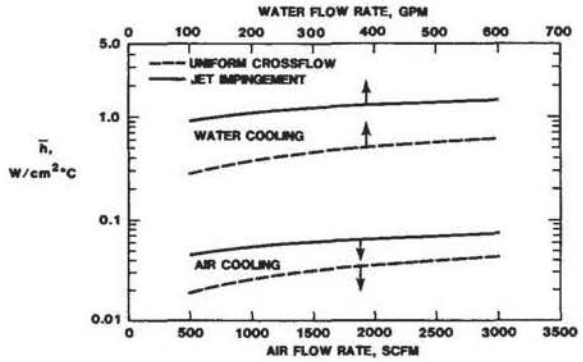

Fig. 15—Mean PDC cutter heat transfer coefficients under typical air and water drilling conditions.

response function data of Table 2 suggest that cooling rates higher than about 5 W/(cm^2 · °C) [8,800 Btu/(hr-sq ft-°F)] do not further reduce wearflat temperatures significantly; however, this is not a correct interpretation. Since α is a function of f, the product αf should be examined before drawing conclusions about convective cooling. This product is plotted for the baseline case in Fig. 13. Since αf is directly proportional to mean wearflat temperature rise for a given wear condition and cutting speed, it is noted that, at least for lower cutting speeds, convective cooling continues to reduce temperatures substantially for values of h greater than 5 W/(cm^2 · °C) [8,800 Btu/(hr-sq ft-°F)]. It will be shown, however, that higher cooling rates cannot be achieved practically downhole.

Laboratory measurements of convective heat transfer coefficients for a single cutter placed in uniform crossflow of water were reported in earlier work.[4] Such a uniform flow field is an idealized model representing the simple assumption of uniform radial flow of drilling fluid across the face of the bit. In reality, however, the flow field across the face of a PDC bit is turbulent, transient, and contains radial and axial jets.[13] In an effort to obtain an estimate of the heat transfer coefficients in such a flow field, laboratory measurements were conducted for a single worn cutter cooled by a 0.64-cm [0.25-in.] low-

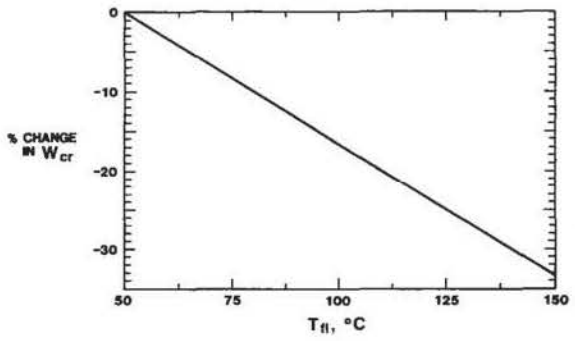

Fig. 16—Effects of downhole fluid temperature (Case 8).

pressure water jet directed at the cutter face. The experimental method is reported in Ref. 19, and the results are shown in Fig. 14. These results are similar to those obtained with a uniform flow field, except that the constants and exponents of the correlations differ in magnitude.

A more useful form of the experimental data is presented in Fig. 15. These curves show the mean heat transfer coefficient over the surface of a cutter cooled by both uniform radial flow and jet impingement, for both air and water. These curves were computed from the experimental correlations, using the following assumptions: (1) for uniform radial flow, the cutter was assumed to be located on the periphery of a 22.2-cm [8.75-in.] bit with 1.5-cm [0.59-in.] standoff between the bit body and the rock; (2) for jet impingement, ten 0.64-cm [0.25-in.] nozzles were assumed for the entire bit; (3) a fluid temperature of 50°C [122°F] was assumed for evaluating all fluid properties. It is seen that mean heat transfer coefficients greater than about 1.5 W/(cm^2 · °C) [2,600 Btu/(hr-sq ft-°F)] for water and 0.075 W/(cm^2 · °C) [130 Btu/(hr-sq ft-°F)] for air cannot be achieved easily. The actual flow field around any given cutter is probably some combination of radial flow and jet impingement.

Downhole Fluid Temperature. As seen in Eqs. 9 and 10, downhole fluid temperature plays a significant role in defining cutter temperature and, hence, critical WOC. To illustrate these effects, the change in W_{cr} from the baseline case for downhole fluid temperatures up to 150°C [302°F] are computed in Case 8. The results, shown in Fig. 16, indicate a substantial reduction in critical WOB. Since downhole fluid temperatures in geothermal drilling can easily exceed 100°C [212°F],[14] it may be desirable in certain cases to precool the drilling fluid at the surface.

Inadequate Rock Chip Removal. As noted earlier, the diamond layer plays a major role in transferring heat away from the cutter wearflat. Thus, convection at the diamond surface is critical, especially that portion near the wearflat. When cutting rock, this lower portion of the cutter face may be insulated effectively from the cooling fluid by inadequate removal of rock chips as they are formed. Such could be the case if proper hydraulics are not used.

To simulate this effect, the boundary conditions on the diamond surface were changed in Case 9. The lower por-

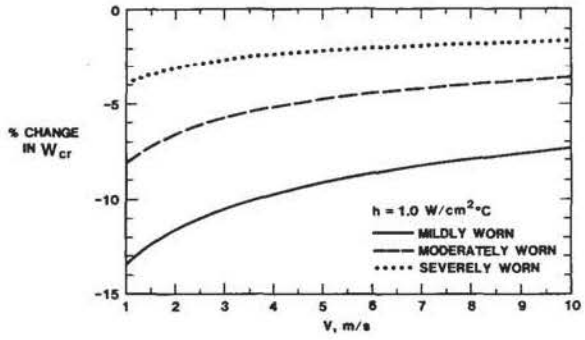

Fig. 17—Effects of insulating lower half of diamond face from cooling fluid: Case 9, $h = 1.0$ W/(cm^2 · °C).

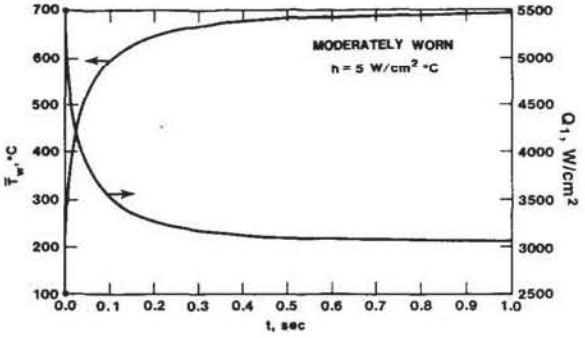

Fig. 19—Transient thermal response for beginning of drilling.

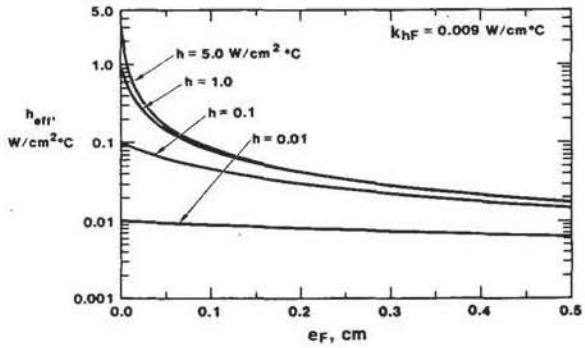

Fig. 18—Effects of bit balling on effective cooling rate.

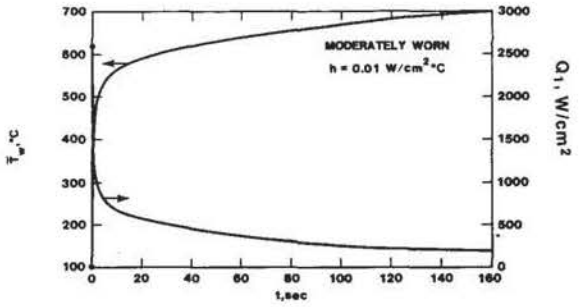

Fig. 20—Transient thermal response for beginning of drilling.

tion (up to 50%) of the diamond face was modeled as adiabatic for each wear condition. The results are shown in Fig. 17 for a typical water cooling rate. With a mildly worn cutter, a buildup of rock chips in front of the cutter can effectively reduce critical WOC by up to 13% at $v = 1$ m/s [3.3 ft/sec].

Bit Balling. Bit balling, where the cutters become surrounded by crushed rock debris, is a common occurrence with PDC bits, although experience has shown that it can be overcome with proper hydraulic design and operating conditions.[15] The detrimental effects of bit balling include reduced penetration rate and increased cutter temperatures.

The thermal effects of bit balling arise from an increase in the thermal resistance to heat flow from the cutter surface to the cooling fluid. With no bit balling, the thermal resistance for an elemental area on the cutter surface is

$$R = \frac{1}{h\ dA}. \quad \ldots\ldots\ldots\ldots\ldots\ldots\ldots\ldots\ldots\ldots (13)$$

With bit balling, heat flow from the cutter surface must pass through a layer of saturated rock debris. This increases the thermal resistance to

$$R = \frac{1}{h\ dA} + \frac{e_F}{k_{hF}\ dA}, \quad \ldots\ldots\ldots\ldots\ldots\ldots\ldots\ldots (14)$$

where e_F is the thickness and k_{hF} is the thermal conductivity of the rock debris surrounding the cutter. An effective convective heat transfer coefficient, h_{eff}, can be defined for bit balling by the following equation:

$$R = \frac{1}{h_{\text{eff}}\ dA}. \quad \ldots\ldots\ldots\ldots\ldots\ldots\ldots\ldots\ldots\ldots (15)$$

Substituting Eq. 15 into Eq. 14 gives the final result

$$h_{\text{eff}} = \frac{hk_{hF}}{k_{hF} + he_F}. \quad \ldots\ldots\ldots\ldots\ldots\ldots\ldots\ldots\ldots\ldots (16)$$

This relation is plotted in Fig. 18 for the assumed value of k_{hF} equal to the thermal conductivity of shale.[12] Note that under conditions of high cooling, a significant reduction in cutter cooling is experienced with very thin layers of rock debris. This emphasizes the need to prevent bit balling if maximum cutter life is to be obtained.

Transient Effects on Wearflat Temperature

With a transient event such as lifting the bit off bottom to make a connection, the numerical boundary condition at the wearflat changes simply from frictional heating to convective cooling. With more complex events, such as bit bounce and beginning drilling after making a connection, the cutter wearflat heat flux becomes a function of

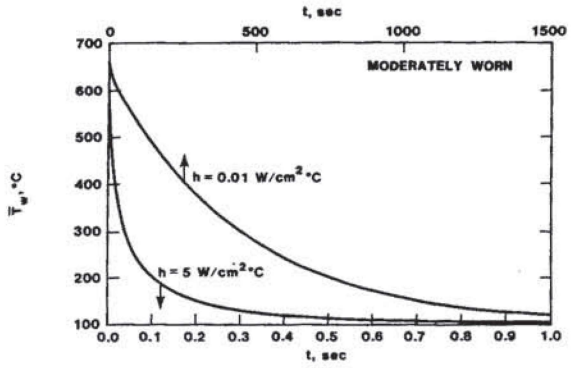

Fig. 21—Transient thermal response caused by lifting bit off bottom.

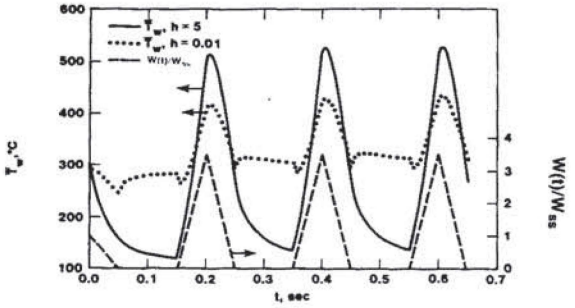

Fig. 22—Transient thermal response caused by bit bounce (moderately worn cutter).

time. An expression for this heat flux may be obtained by substituting Eq. 6 into Eq. 2, with the result

$$Q_1 = \frac{K_f W v}{A_w} - (\bar{T}_w - T_{fl}) \frac{3\sqrt{\pi}}{4} k_h)_2 \left(\frac{v}{\alpha_f L}\right)^{1/2}, \quad (17)$$

where $\bar{T}_w$ is now a function of time.

Since $\bar{T}_w$ is a function of Q_1, the exact solution of Eq. 17 would require numerical iteration; however, an approximate solution for Q_1 at time t may be obtained by evaluating $\bar{T}_w$ at time $t-\Delta t$. This approach produces accurate results if the timestep Δt is small.

Beginning To Drill. To illustrate the effects of beginning to drill, a transient numerical analysis was conducted in Case 10. The moderately worn cutter initially was assumed to have a uniform temperature equal to an assumed downhole fluid temperature of 100°C [212°F]. Frictional heating at the wearflat was begun at time $t=0$, the value of which was determined from Eq. 17. The value of the product $K_f W v$ was set to the value that produces a steady-state wearflat temperature of 700°C [1,292°F].

The results are shown in Fig. 19 for a high cooling rate, $h=5.0$ W/(cm^2 · °C) [8,800 Btu/(hr-sq ft-°F)], and in Fig. 20 for a low cooling rate, $h=0.01$ W/(cm^2 · °C) [18 Btu/(hr-sq ft-°F)]. Note that in both cases the cutter wearflat heat flux Q_1 rapidly decreases from its initially high rate as the cutter temperature increases, and the rock absorbs a larger fraction of the frictional heat. Note also that the cutter takes much longer to reach steady-state temperatures with the low cooling rate than with the high one. With high cooling rates, a higher heat flux is required to achieve the steady-state wearflat temperature, and therefore, the cutter responds more quickly.

Lifting the Bit Off Bottom. The transient effects of lifting the bit off bottom to make a connection are studied in Case 11 and illustrated in Fig. 21. Here, the cutters were assumed to have initial temperature distributions equal to those achieved with steady-state wearflat temperatures of 700°C [1,292°F]. At time $t=0$, the wearflat boundary condition was changed to convective cooling. Note that with high cooling rates, the wearflat temperature again responds very quickly, whereas with low cooling rates, it takes a relatively long time for the cutter to cool down to the fluid temperature. These results are used in a later section to compute thermal stresses resulting from these environmental conditions.

Bit Bounce. Downhole measurements of drillstring motion have shown that under conditions associated with "rough drilling" in hard rock, severe longitudinal and torsional vibration of the drillstring can cause the bit to actually bounce off bottom for part of the vibration cycle.[16] Such an extreme situation occurs when the natural frequency of the drillstring matches the frequency of the excitation force. This excitation force, in the case of three-cone rock bits, arises from a three-lobed bottomhole pattern that develops and becomes self-sustaining under certain conditions in hard rock. Whether or not a similar condition develops with PDC bits has not yet been determined.[17] If it does, however, the thermal effects of bit bounce can be shown to the highly detrimental to bit life.

In Case 12, a moderately worn cutter was assumed to be drilling with a constant WOC that produces an initial steady-state wearflat temperature of 300°C [572°F]. With a low cooling rate, $h=0.01$ W/(cm^2 · °C) [18 Btu/(hr-sq ft-°F)], the required steady-state WOC is less than one-half that required with improved cooling, $h=5.0$ W/(cm^2 · °C) [8,800 Btu/(hr-sq ft-°F)]. At time $t=0$, bit bounce was assumed to begin suddenly. The computed wearflat temperatures for the two cooling rates are shown in Fig. 22, together with the assumed transient WOC behavior. This behavior was modeled from downhole force measurements[16] for a particular run that showed a maximum bit load of 3.5 times the mean bit weight and a bit bounce frequency of 5 cycles per second.

The high inertial loading associated with bit bounce causes transient wearflat temperatures to exceed 500°C [932°F] with high cooling rates and 400°C [752°F] with low rates. Since these temperatures are achieved during the part of the cycle in which the cutter is in contact with the rock, extremely high wear rates would be expected during those periods. The conclusion is that even if the bit is being run at or below the steady-state critical WOB, unacceptably high wear rates may occur if the bit starts bouncing, assuming that a PDC bit could even survive the mechanical stress caused by impact loading. The rapid thermal response of cutters to changes in bit weight further suggests that undesired excursions in wearflat temperature may occur even in instances where the bit

TABLE 4—STRUCTURAL MATERIAL PROPERTIES

	Temperature			
	Tungsten Carbide		Diamond	
	(20°C)	[1000°C]	(20°C)	[1000°C]
Young's modulus, GPa	524.0	205.0	841.0	841.0
Poisson's ratio	0.26	0.26	0.26	0.26
Yield stress, GPa	0.69	0.169	6.90	6.90
Hardening modulus, GPa	293.0	293.0	100.0	100.0
Thermal expansion coefficient, 10^{-6}/°C	6.0	6.0	3.2	3.2

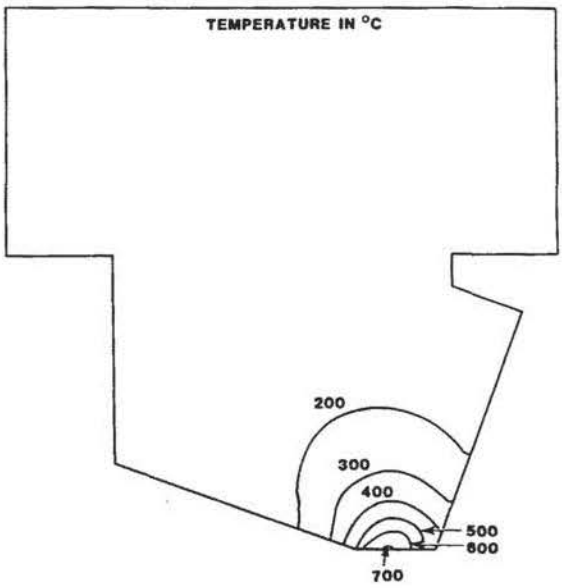

Fig. 23—Thermal contours at the end of the frictional heating phase, $h = 5.0$ W/(cm^2·°C).

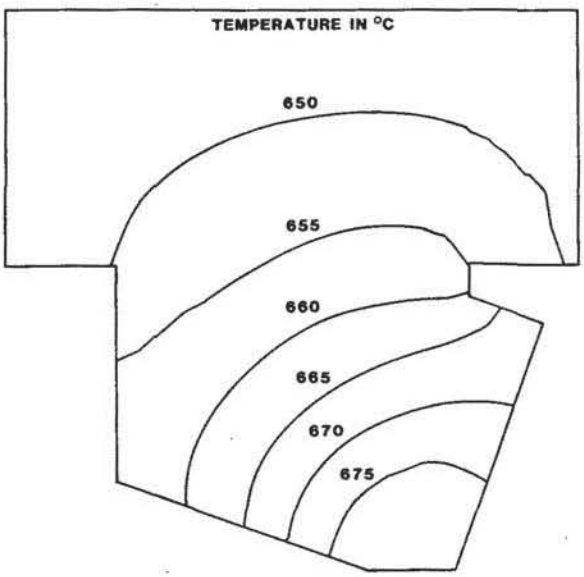

Fig. 24—Thermal contours at the end of the frictional heating phase, $h = 0.01$ W/(cm^2·°C).

weight merely fluctuates without full bounce. Therefore, under conditions known to cause rough drilling, it may be advisable to employ shock subs or other drillstring design modifications[17] with PDC bits to reduce or eliminate bit weight fluctuations.

Thermal Stresses Induced in PDC Cutters

Structural Analysis. The final phase of this work was a preliminary determination of the thermal stresses induced in a cutter by the previously computed thermal environments. The structural analysis of the moderately worn cutter was preformed using a general purpose nonlinear finite element program.[18] The cutter geometry was discretized into 2D planar finite elements similar to those shown in Fig. 2. The cutter physical dimensions are such that a plane-stress formulation is necessary. Although this formulation is felt to be adequate for this study, a three-dimensional model of the cutter would be desirable.

The model boundary conditions were chosen to simulate the mechanical restraint provided by the bit body upon the carbide stud. The vertical boundaries of the bit body segment surrounding the stud were assumed to be fixed. Generally, there are cutting and vertical forces that act on the cutter in addition to the thermal loads. The contributions of these mechanical forces have been omitted from the current analyses because our intent was to study thermal effects on the cutter. Future studies[19,20] will include mechanical loads to evaluate cutter integrity. The initial stress-free temperature for the cutter was assumed to be the downhole fluid temperature.

The thermal environments assumed for the stress calculations discussed in this paper are those associated with the transient frictional heating, resulting from the start of drilling, and the wearflat convective cooling, resulting from the lifting the bit off bottom to make a connection. Temperature gradients were computed for every element in the cutter at each timestep of these transient thermal analyses. These gradients were used to compute the equivalent thermal forces applied to each element.

An important part of the structural analysis was the determination of the WC-Co and diamond material properties, especially the WC-Co material property variation with temperature. Elastic modulus and yield stress are affected by temperature variation. The elastic modulus for WC-Co was assumed to decrease with increased temperature in the same manner as the material hardness.[9] Yield stress was assumed to decrease to approximately 25% of its room temperature value at 1000°C [1,832°F]. These variations with temperature are given in Table 4. The value of the postyield hardening modulus

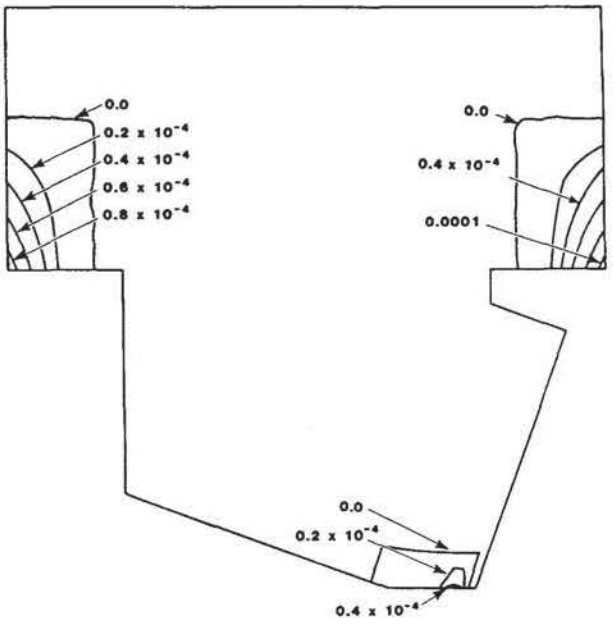

Fig. 25—Plastic strain contours at the end of the cooling phase, $h = 5.0$ W/(cm^2 · °C).

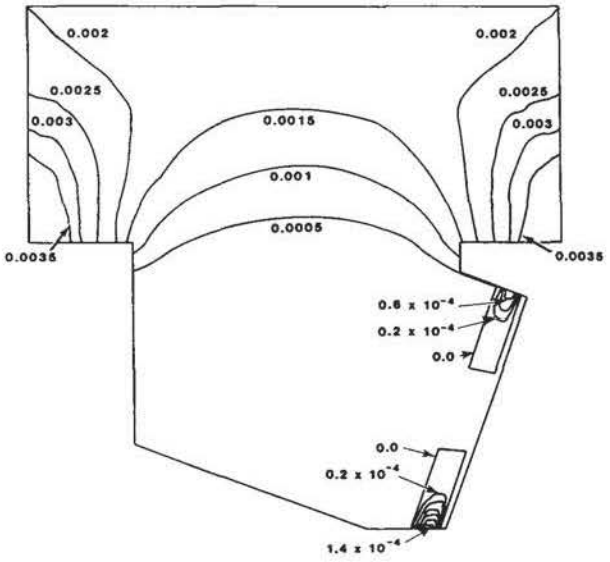

Fig. 26—Plastic strain contours at the end of the cooling phase, $h = 0.01$ W/(cm^2 · °C).

was assumed constant with temperature. The diamond cutter face was modeled as an elastic-plastic material whose properties do not vary with temperature. Since a nonlinear material variation was assumed for this problem, an accurate history of the material response was necessary for the solution. The thermal histories thus were broken into small temperature increments to provide the accurate thermal loads required for each analysis.

Structural Analysis Results. A comparison was made between the thermal stress results obtained for the high and low cooling rates assumed in Cases 10 and 11. Temperature distributions in the cutter at the end of the wearflat heating phase for both cutter cooling rates are shown in Figs. 23 and 24. By this time in the thermal analysis, the cutter has reached steady state, with mean wearflat temperatures of 700°C [1,292°F]. Note that there are steep thermal gradients near the wearflat for the high cooling rate, while the temperature is fairly uniform for the low cooling rate. This inherent difference causes different thermal stress behavior for the two cooling rates.

The effective plastic strain contours at the end of the wearflat cooling phase are shown in Figs. 25 and 26. The yielding of the diamond layer and WC-Co compact seen in these figures was found to occur for both cooling rates during the heating phase of the analysis, with no additional yielding occurring during the cooling phase. The maximum plastic strain for the high cooling rate occurs near the wearflat. For the low cooling rate, there are two regions of yielding at the interface between the WC-Co compact and the diamond layer. The first and largest region occurs near the wearflat, and the second occurs at the top of the compact. The maximum plastic strains in this region for the low cooling rate are over three times higher than the maximum strains achieved with improved cooling. Yielding also is seen to occur in the bit body near the vertical boundaries, owing to the fixed boundary restraint assumed at these surfaces. At the low cooling rate, this assumed restraint also causes yielding in the neck of the cutter stud, where relatively high temperatures are observed.

The mechanism that causes the large plastic yielding in the compact region at the low cooling rate appears to be the cumulative differential thermal expansion between the WC-Co and the diamond at the high temperatures. This would explain the yielding at both the top and the bottom of the compact. This mechanism would not be as prevalent for the high cooling rate because the temperatures along the WC-Co/diamond interface are much lower. Instead, the yielding at the high cooling rate appears to result from the steep thermal gradients present at the wearflat. Studies of other wear configurations indicate that the thermal gradient increases with the size of the wearflat, so greater yielding is expected as the cutter wears. These studies are aimed at identifying the conditions under which PDC cutters are susceptible to thermal stress cracking, such as that which has been observed in the field.[3,7]

Conclusions

1. A method has been developed for predicting mean wearflat temperatures of PDC cutters under simulated steady-state and transient downhole conditions. The method has been shown to produce results that compare favorably with available experimental data.

2. Cutter wear rates correlate with mean wearflat temperatures, and available experimental data indicate greatly increased wear rates above 350°C [662°F].

3. A relation has been developed for determining the critical WOB, above which gauge cutter wearflat temperatures exceed 350°C [662°F].

4. The use of WC-Co grades with lower thermal conductivities for cutter studs and bit bodies does not increase wearflat temperatures significantly; the use of such grades for the WC-Co compact bonded to the diamond, however,

can lead to significant increases in temperatures and reductions in the critical WOB.

5. A diamond layer thickness twice that conventionally used can significantly increase the WOB that can be tolerated by mildly worn cutters.

6. Efforts to design fluid ports for increased cooling of the bit body or internal cooling of cutter studs are not worthwhile, since they do not reduce wearflat temperatures significantly.

7. Formation characteristics have a significant effect on cutter wearflat temperatures. Owing to the large range of friction coefficient and rock thermal conductivity that may be encountered in normal drilling practice, actual downhole cutter temperatures cannot be predicted accurately unless specific data on formation characteristics are obtained.

8. Within the range of cutter cooling rates achievable in practice, increased cooling rates lead to significant reductions in wearflat temperatures.

9. Even minor bit balling substantially reduces effective cutter cooling rates.

10. Bit bounce resulting from drillstring vibration can significantly increase cutter temperatures from their steady-state values during the critical fraction of the cycle when the cutters are in contact with the rock.

11. Thermal stresses induced in cutters under downhole conditions can reach levels high enough to cause yielding of the cutting structure.

Nomenclature

dA = elemental area on cutter surface, cm^2 [sq in.]
A_w = cutter wearflat area, cm^2 [sq in.]
C = cutter material specific heat, kJ/(kg·°C) [Btu/(lbm-°F)]
C_f = rock specific heat, kJ/(kg·°C) [Btu/(lbm-°F)]
C_{fl} = fluid specific heat, kJ/(kg·°C) [Btu/(lbm-°F)]
d = cutter stud diameter, cm [in.]
e_F = thickness of rock debris surrounding cutter, cm [in.]
f = thermal response function (Eq. 7), (cm·°C)/W [(sq ft-hr-°F)/Btu]
h = convective heat transfer coefficient, $W/(cm^2 \cdot °C)$ [Btu/(hr-sq ft-°F)]
$\bar{h}$ = mean convective heat transfer coefficient, $W/(cm^2 \cdot °C)$ [Btu/(hr-sq ft-°F)]
h_{eff} = effective heat transfer coefficient with bit balling, $W/(cm^2 \cdot °C)$ [Btu/(hr-sq ft-°F)]
k_h = cutter material thermal conductivity, $W/(cm^2 \cdot °C)$ [Btu/(hr-ft-°F)]
k_{hf} = rock thermal conductivity, $W/(cm^2 \cdot °C)$ [Btu/(hr-ft-°F)]
k_{hF} = rock debris thermal conductivity, W/(cm·°C) [Btu/(hr-ft-°F)]
k_{hfl} = fluid thermal conductivity, W/(cm·°C) [Btu/(hr-ft-°F)]
K_f = friction coefficient between cutter and rock
L = cutter wearflat length, cm [in.]
n = number of cutters on bit
N_{Nu} = Nusselt number $= hd/k_{hfl}$
N_{Pr} = Prandtl number $= C\rho_{fl}/k_{hfl}$
N_{Re} = Reynolds number $= \rho_{fl} du/\eta_{fl}$
q = fluid flow rate, L/s [gal/min]
Q = total wearflat frictional heat flux (Eq. 1), W/cm^2 [Btu/(hr-sq ft)]
Q_1 = frictional heat flux into cutter, W/cm^2 [Btu/(hr-sq ft)]
Q_f = frictional heat flux into rock, W/cm^2 [Btu/(hr-sq ft)]
R = thermal resistance from cutter surface to fluid, °C/W [(hr-°F)/Btu]
t = time, seconds
$\bar{T}_w$ = mean cutter wearflat temperature, °C [°F]
T_{fl} = fluid temperature, °C [°F]
$\bar{T}_s$ = mean rock surface temperature beneath cutter, °C [°F]
T_f = bulk rock temperature, °C [°F]
u = fluid jet velocity, m/s [ft/sec]
v = cutting speed, m/s [ft/sec]
W = weight on cutter, N [lbf]
W_{cr} = critical weight on cutter, N [lbf]
W_{ss} = steady-state weight on cutter, N [lbf]
α = energy partitioning fraction $= Q_1/(Q_1+Q_f)$
α_f = rock thermal diffusivity, $k_{hf}/\rho_f C_f$
η_{fl} = fluid dynamic viscosity, Pa·s [cp]
ρ = cutter material density, g/cm^3 [lbm/cu ft]
ρ_f = rock density, g/cm^3 [lbm/cu ft]
ρ_{fl} = fluid density, g/cm^3 [lbm/cu ft]

Subscripts

i = initial
ss = steady state
cr = critical

References

1. van Prooyen, J., Juergens, R., and Gilbert, H.E.: "Recent Field Results with New Bits," *J. Pet. Tech.* (Sept. 1982) 1938–46.
2. Keller, W.S. and Crow, M.L.: "Where and How Not to Run PDC Bits," paper SPE 11387 presented at the 1983 IADC/SPE Drilling Conference, New Orleans, Feb. 20–23.
3. Arceneaux, M.A. and Fielder, J.L.: "Field Experience with PDC Bits in Northeast Texas," paper SPE 11390 presented at the 1983 IADC/SPE Drilling Conference, New Orleans, Feb. 20–23.
4. Ortega, A. and Glowka, D.: "Frictional Heating and Convective Cooling of Polycrystalline Diamond Drag Tools During Rock Cutting," *Soc. Pet. Eng. J.* (April 1984) 121–28.
5. Jaeger, J.C.: "Moving Sources of Heat and the Temperature at Sliding Contacts," *Proc.*, Royal Soc. New S. Wales (1942) **76**, 203–24.
6. Gartling, D.K.: "COYOTE—A Finite Element Computer Program for Nonlinear Heat Conduction Problems," Sandia Report No. SAND77-1332 (Revised), Sandia Natl. Laboratories, Albuquerque (Oct. 1982).
7. Hibbs, L.E. and Sogoian, G.C.: "Wear Mechanisms for Polycrystalline Diamond Compacts as Utilized for Drilling in Geothermal Environments—Final Report," Sandia Report No. SAND82-7213, May 1983.
8. Lee, M. and Hibbs, L.E. Jr.: "Role of Deformation Twin Bands in the Wear Processes of Polycrystalline Diamond Tools," *Wear of Materials*, K.C. Ludema, W.A. Glaeser, and S.K. Rhee (eds.), ASME (1979) 485–91.
9. Selcuk, S.: "Analysis of Coefficient of Rock Strength and Measurement of Percussive Penetration Rates and Bit Wear," MS Thesis, Colorado School of Mines, Golden (Sept. 1981).

10. Trigger, K.J. and Chao, B.T.: "The Mechanism of Crater Wear of Cemented Carbide Tools," *Trans.*, ASME (July 1956) 1119–26.
11. Ling, F.F. and Saibel, E.: "On the Tool-Life and Temperature Relationship in Metal Cutting," *Trans.*, ASME (July 1956) 1113–17.
12. Robertson, E.: "Thermal Conductivities of Rocks," USGS Open-File Report 79-356 (1979).
13. Glowka, D.: "Optimization of Bit Hydraulic Configurations," *Soc. Pet. Eng. J.* (Feb. 1983) 21–32.
14. Mitchell, R.F.: "Downhole Temperature Prediction for Drilling Geothermal Wells," *Proc.*, Intl. Conference on Geothermal Drilling and Completion Technology, Albuquerque (Jan. 1981) 14–1 to 14–18.
15. Radtke, R.P. and Pain, D.D.: "Optimization of Hydraulics for Polycrystalline Diamond Composite Bits in Gulf Coast Shales with Water-Based Muds," *J. Pet. Tech.* (Oct. 1984) 1697–1702.
16. Deily, F.H. *et al.*: "Downhole Measurements of Drill String Forces and Motions," *J. Eng. Ind.* (May 1968) 217–25; *Trans.*, ASME.
17. Dareing, D.W.: "Drill Length Collar Is a Major Factor in Vibration Control," *J. Pet. Tech.* (April 1984) 637–44.
18. *MARC-CDC User Information Manual, Volumes I–III*, General Purpose Finite Element Analysis Program, Pub. No. 17309500, Control Data Corp., Minneapolis (1977).
19. Glowka, D. and Stone, C.M.: "The Thermal Limitations of Polycrystalline Diamond Compact Drag Bits in Geothermal Drilling," Sandia Report No. SAND83-1533, Sandia Natl. Laboratories, Albuquerque; in preparation.
20. Glowka, D.A. and Stone, C.M.: "Effects of Thermal and Mechanical Loading on PDC Bit Life," paper SPE 13257 presented at the 1984 SPE Annual Technical Conference and Exhibition, Houston, Sept. 16–19.

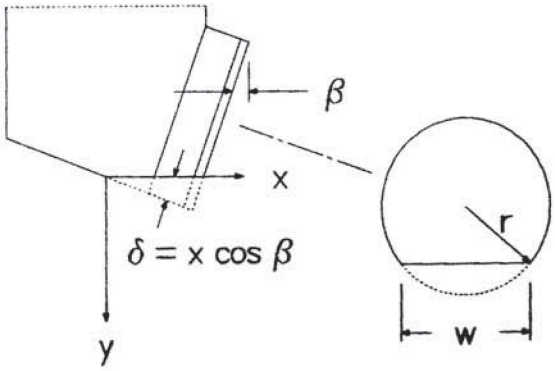

Fig. A-1—Schematic of worn cutter, showing pertinent geometric parameters.

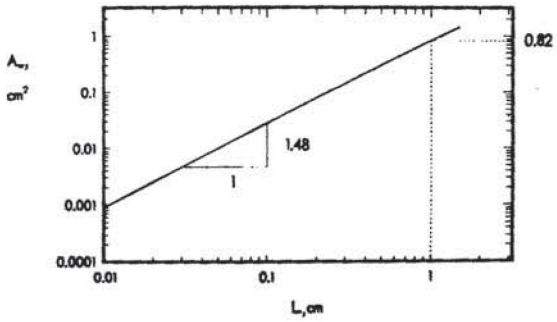

Fig. A-2—Plot of Eq. A-5.

Acknowledgment

This work was performed under the auspices of U.S. DOE Contract No. DE-AC04-76DP00789.

APPENDIX

As shown in Fig. A-1, the cutter wearflat may be modeled as a planar surface that passes through a cylinder at an angle, $\beta=20°$, with respect to the axis of the cylinder. An elemental area on the wearflat is given by

$$dA_w = w\,dx, \quad \ldots\ldots\ldots\ldots\ldots\ldots\ldots\ldots\ldots\ldots (A\text{-}1)$$

where

$$w = 2[r^2-(r-\delta)^2]^{1/2}$$

$$= 2[r^2-(r-x\,\sin\beta)^2]^{1/2}$$

$$= 2(2rx\,\sin\beta - x^2\,\sin^2\beta)^{1/2}. \quad \ldots\ldots\ldots\ldots\ldots (A\text{-}2)$$

Thus,

$$A_w = 2\,\sin\beta \int_0^L (2C_1x - x^2)^{1/2}\,dx, \quad \ldots\ldots\ldots\ldots (A\text{-}3)$$

where $C_1 = r/\sin\beta$.

Integrating and applying the limits give the final result:

$$A_w = \sin\beta\{(L-C_1)(2C_1L-L^2)^{1/2} + C_1^2[\sin^{-1}$$

$$\cdot(L/C_1-1)+\pi/2]\}. \quad \ldots\ldots\ldots\ldots\ldots\ldots (A\text{-}4)$$

For the geometry of interest, $\beta=20°$ and $r=0.66$ cm [0.26 in.]. As seen in Fig. A-2, this equation is linear in log-log space; thus, the simplified equation for the wearflat length is

$$A_w = 0.82L^{1.48}. \quad \ldots\ldots\ldots\ldots\ldots\ldots\ldots\ldots (A\text{-}5)$$

SI Metric Conversion Factors

Btu	×	1.055 056	E+00	= kJ
Btu/hr	×	2.930 711	E−01	= W
cp	×	1.0*	E−03	= Pa·s
cu ft	×	2.831 685	E−02	= m^3
ft	×	3.048*	E−01	= m
°F		(°F−32)/1.8		= °C
gal	×	3.785 412	E−03	= m^3
in.	×	2.54*	E+00	= cm
sq in.	×	6.451 6*	E+00	= cm^2

*Conversion factor is exact.

SPEJ

Original manuscript received in the Society of Petroleum Engineers office Oct. 5, 1983. Paper accepted for publication Feb. 16, 1984. Revised manuscript received May 21, 1984. Paper (SPE 11947) first presented at the 1983 SPE Annual Technical Conference and Exhibition held in San Francisco, Oct. 5–8.